Role of Lateral Interactions in Adsorption Kinetics: CO/Rh{100}

Rickmer Kose, Wendy A. Brown,† and David A. King*

Department of Chemistry, University of Cambridge, Lensfield Road, Cambridge CB2 lEW, United Kingdom, and Department of Chemistry, University College London, 20 Gordon Street, London WC1H 0AJ, United Kingdom

Received: April 26, 1999; In Final Form: August 11, 1999

The coverage-dependent heats of adsorption and sticking probabilities for CO on Rh{100} were measured. The initial heat is 118 ± 4 kJ mol^{-1}, with an initial sticking probability of ∼0.87; the saturation coverage is ∼0.8 monolayer. By means of a Kisliuk fit to the sticking probability data, the transition between the two main adsorbate phases (c(2×2) structure at 0.5 monolayer and p(4$\sqrt{2}$×$\sqrt{2}$)*R*45° structure at 0.75 monolayer) could be detected, allowing the determination of two independent Kisliuk parameters for the first ($K = 0.3$) and second ($K = 1$) regime. The differential heat data was successfully reproduced by means of a Monte Carlo simulation. A discrete CO−CO interaction potential was implemented and optimized, giving CO−CO interaction energies of $E_{nn} = 9 \pm 1$ kJ mol^{-1} (nearest neighbor), $E_{nnn} = 1 \pm 0.5$ kJ mol^{-1} (next-nearest neighbor) and $E_{nnnn} = -1 \pm 0.5$ kJ mol^{-1} (next-next-nearest neighbor). These energies agree well with the experimentally determined *nn* and *nnn* interaction energies and with a calculated CO−CO interaction potential (DFT) for CO on Pt{111}.

1. Introduction

The adsorption and oxidation properties of CO at rhodium surfaces have received much interest in the past, and with the increasing use of rhodium as a component of the car exhaust catalyst, further interest has been recently stimulated.

Here we present the first accurate measurements of the dependence of both the sticking probability and the calorimetric adsorption heat as a function of coverage for CO on a rhodium single-crystal plane, Rh{100}. The experiments were performed using the unique single-crystal adsorption calorimeter at Cambridge which combines absolute measurements of sticking probabilities, calorimetric heats, and surface coverage, and which has been shown to be the most accurate source of these properties for a wide range of adsorbate/substrate systems.[1]

Low-energy electron diffraction (LEED), high-resolution electron energy loss spectroscopy (HREELS), temperature-programmed desorption (TPD), and X-ray photoelectron spectroscopy (XPS) studies all found a c(2×2) structure at low CO coverages (0.5 monolayer),[2−6] and a p(4$\sqrt{2}$×$\sqrt{2}$)*R*45° structure at higher coverages (0.75 monolayer).[5−9] For a coverage of 0.83 monolayer, the formation of a "split" (1×2) structure was reported by Castner et al.,[3] which is attributed to multiple diffraction from an incommensurate hexagonal CO layer.[6] When adsorbing CO at 270 K, Baraldi et al. found that this high-coverage phase produces a third TPD peak, at a desorption temperature of ∼330 K, in addition to the previously observed desorption states at ∼490 and ∼400 K.[5]

Furthermore, Baraldi et al. investigated the evolution of the preexponential and activation energy for desorption as a function of CO coverage. At zero coverage, the activation energy for desorption is 140 kJ mol^{-1}, with a preexponential of $10^{13.5}$ s^{-1}. With increasing CO coverage, the exponent of the preexponential factor drops linearly to a value of 9.5 at saturation (0.83 monolayer). At the same time, the activation energy for desorption drops almost linearly to 70 kJ mol^{-1} at saturation.[5] This essentially agrees with findings of Kim et al. who determined the activation energy for desorption in the zero coverage limit to be 134 kJ mol^{-1}, with a preexponential of 8.4×10^{12} s^{-1}.[9] Using the Chan−Aris−Weinberg method for TPD analysis,[10,11] de Jong and Niemantsverdriet determined the activation energy for desorption to be 131 ± 4 kJ mol^{-1}, with a preexponential factor of $(4 \pm 3) \times 10^{16}$ s^{-1}. The activation energy for desorption shows a good match with previous investigations; however, no account for the discrepancy with previously determined preexponential factors is given.[6] Additionally, the CO coverage as a function of exposure was measured to extract Kisliuk parameters by fitting the uptake curve to a Kisliuk type function,[12] giving $K = 0.7$ ($K = 1$ denotes direct adsorption), and an initial sticking probability of ∼0.75 (however, with unknown error bars).

2. Experimental Section

The experiments were carried out using the Cambridge Single Crystal Adsorption Calorimeter (SCAC) developed in these laboratories, in an ultra-high-vacuum chamber with a base pressure of $\leq 7 \times 10^{-11}$ mbar. CO was adsorbed at room temperature using a pulsed molecular beam[13] (50 ms pulse width, 2.5 s repetition period, $\sim 2 \times 10^{12}$ molecules per pulse). To achieve a measurable change in crystal temperature upon adsorption, the crystal heat capacity is kept low by employing single crystals that are approximately 200 nm thick. The temperature is remotely monitored using a commercially available mercury cadmium telluride (MCT) infrared detector. Typically, the initial adsorption of a single pulse of gas leads to a temperature rise of ∼0.1 K at the crystal surface with a S/N ratio of the amplified infrared signal of ∼100:1.

Parallel to the heat measurements, sticking probabilities were determined using the King and Wells method,[14] which involves

* Corresponding author. Fax: (+44) 1223 336 362. E-mail: eld1000@cam.ac.uk.
† University College London.

10.1021/jp991339e CCC: $18.00
Published on Web 09/28/1999

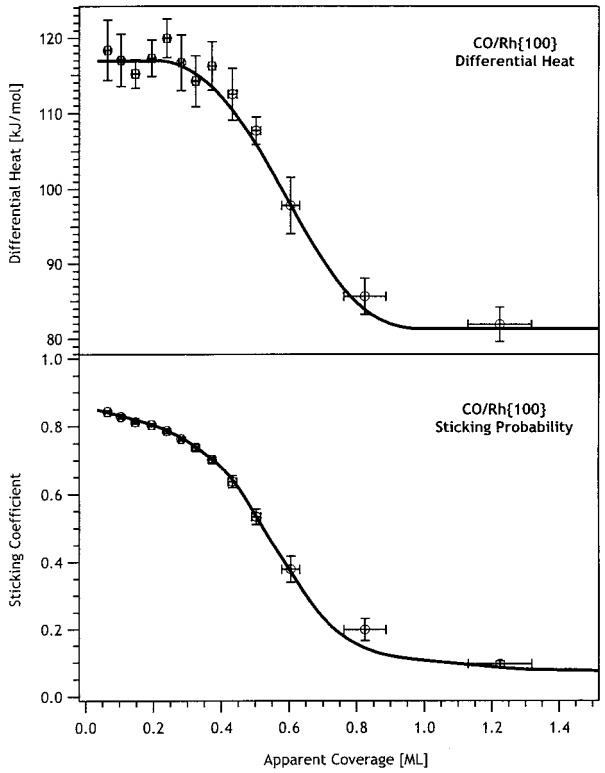

Figure 1. Coverage-dependent differential heat of adsorption (top) and sticking probability (bottom) for CO on Rh{100} adsorbed at 300 K. Open circles are averaged experimental data points, and the solid line represents a smoothing spline through these points, serving as a guide to the eye.

measuring the fraction of an impinging gas pulse which is reflected from the surface. We use the term "apparent coverage" for the presentation; it refers to the coverage determination via integration of successive pulse-dependent sticking probabilities. Any species desorbing between pulses cannot be detected and will thus indefinitely extend the coverage scale when close to or at adsorption−desorption equilibrium. We stress, however, that the coverages are absolutely determined, and for coverages where the adsorption heat is $\geq$100 kJ mol^{-1}, and the desorption rate is negligible, the coverage scale is accurate. The sticking probability and the adsorption heat measured at steady state are referred to as the "steady state sticking coefficient" and the "steady state heat", rcspectively. A detailed description of the experiment and principles can be found elsewhere.[13,15]

Cleaning of the Rh{100} crystal was achieved via Ar ion sputtering at discharge currents below 8 μA and subsequent annealing to ~700 K. Crystal cleanliness and structure were checked using Auger electron spectroscopy (AES) and LEED.

3. Results

The coverage-dependent heat of adsorption for CO on Rh{100} is shown in Figure 1 (top), and the corresponding coverage-dependent sticking probability is given in Figure 1 (bottom). The initial heat of adsorption is 118 ± 4 kJ mol^{-1}, with an initial sticking probability of ~0.87. Up to a coverage of ~0.4 monolayer, the adsorption heat remains practically constant, but then quickly drops to its saturation value of 80 ± 5 kJ mol^{-1}, at a saturation coverage of ~0.8 monolayer. At the same time, the sticking probability drops in a monotonic, nonlinear fashion, to its steady state value of ~0.1, indicating the same saturation coverage as the heat (~0.8 monolayer).

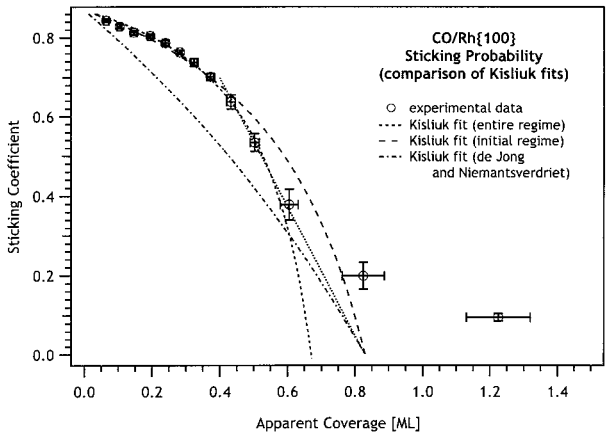

Figure 2. Comparison of Kisliuk fits for the description of the sticking probability of CO on Rh{100}. The original data points are shown as open circles, and the additional curves represent the various Kisliuk fits referred to in the text.

4. Analysis and Discussion

4.1. Adsorption Kinetics. The shape of the sticking probability curve in Figure 1 is strongly indicative of precursor-mediated adsorption, where a CO molecule striking a filled site is trapped into an extrinsic "precursor" state above the chemisorbed state, from which it can hop, and hence has the possibility of arriving at an empty site, before it desorbs.

To compare with previous experiments and to investigate the relevance of precursor-mediated adsorption, Kisliuk fits[12] have been applied to the sticking probability curve (see Figure 2):

$$s(\Theta) = s_0\left(1 + \frac{\Theta/\Theta_s}{1 - \Theta/\Theta_s}K\right)^{-1}, \quad (0 \leq K \leq 1) \qquad (1)$$

Here, the coverage-dependent sticking probability $s(\Theta)$ is given in terms of the instantaneous coverage Θ_s, the initial sticking probability s_0, and a parameter K which describes the degree of mobility of the adsorption precursor. Small values of K indicate a highly mobile precursor, while $K = 1$ corresponds to a totally immobile precursor and hence simple Langmuir adsorption kinetics.

There are in effect two variable fitting parameters in eq 1, K and the saturation coverage, or number of available CO sites, N_s. Fitting the major part of the sticking probability curve, corresponding to the regime up to $\Theta \simeq 0.6$ monolayer, where reversible adsorption begins since the heat falls below 100 kJ mol^{-1}, with this expression results in the curve (short dash) shown in Figure 2, where the corresponding Kisliuk parameter is $K = 0.2$, with an initial sticking probability of 0.87 and a saturation coverage of 0.67. The dash-dot-dash line represents the results found by de Jong and Niemantsverdriet,[6] bearing little relation to the actual measured curve. Their investigations were based on an indirect measurement of sticking probabilities, involving an initial sticking probability of αs_0, where $s_0 = 0.75$ and α accounts for the unknown accuracy of their pressure measurement. For comparison in Figure 2, α was adjusted so that their initial sticking probability coincides with our measurements, and the resulting value for α is 1.1.

The differential heat of adsorption curve (Figure 1, top) maintains a practically constant heat of adsorption for coverages up to ~0.4 monolayer. For coverages above 0.4 monolayer, the adsorption heat drops rapidly, probably due to an ordering of the adsorbate layer to a c(2×2) structure, changing its capability of accommodating additional adsorbates, leading to the observed drop in heat and sticking probability. Taking this model into

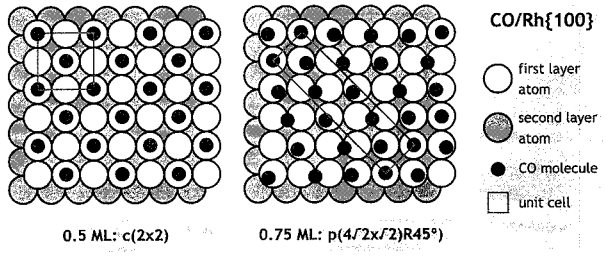

Figure 3. Structure models for CO adsorbed on Rh{100}, after de Jong and Niemantsverdriet.[6]

account, and assuming that precursor-mediated adsorption only plays an important role for coverages below 0.4 monolayer, a revised Kisliuk fit has to be applied to the sticking probability, taking into consideration the saturation coverage of 0.83 monolayer, and is shown as the curve (long dash) in Figure 2. The Kisliuk parameter from this fit is determined to be $K = 0.3$, again indicating a mobile precursor state upon adsorption (we attach no particular significance to the *values* of *K* obtained). The remaining part of the sticking probability curve can be well fitted with a linear function for coverages above 0.4 monolayer (dotted curve in Figure 2), showing that at coverages above 0.4 monolayer, the adsorption is entirely determined by direct adsorption, without the presence of intrinsic or extrinsic precursor states. Close to saturation, the measured ("apparent") sticking probability deviates from the linear fit due to species desorbing between pulses.

The change of the adsorption behavior at a coverage of ~0.4 monolayer is in line with the formation of a c(2×2) structure below ~0.5 monolayer, and a restructuring of the adsorbate layer to a p($4\sqrt{2}\times\sqrt{2}$)*R*45° phase at higher coverages.[2−9] For the low-coverage phase, CO adsorbs exclusively in on-top sites, whereas for the high-coverage phase, the adsorbates occupy a mixture of bridge and on-top sites.[5,6] Figure 3 illustrates the corresponding structural models proposed by de Jong and Niemantsverdriet, based on their LEED, TPD and reflection−absorption infrared spectroscopy (RAIRS) investigations.[6]

4.2. Lateral Interactions. The adsorption of CO on Rh{100} at 300 K has been simulated by means of a Monte Carlo procedure.[16] More details on the particular simulation algorithm implemented here can be found elsewhere.[17] The simulation represents the Rh{100} surface as a square (60 × 60) grid with an interatomic distance[18] of 2.69 Å, permitting on-top adsorption only. A best fit to differential heat of adsorption and sticking probability was achieved with a preexponential factor of 10^{13} s^{-1}, and lateral CO−CO interaction energies of $E_{nn} = 9 \pm 1$ kJ mol^{-1} (nearest neighbor), $E_{nnn} = 1 \pm 0.5$ kJ mol^{-1} (next-nearest neighbor), and $E_{nnnn} = -1 \pm 0.5$ kJ mol^{-1} (next-next-nearest neighbor).

The calculated heat curve and the corresponding experimental data are shown in Figure 4. The simulation takes into account desorption between pulses to simulate the apparent coverage from the experiment; however, this effectively does not happen for coverages below 0.75 monolayer. It is important to note that the simulation makes crude assumptions about the adsorption process and the aforementioned change in the adsorption kinetics at ~0.4 monolayer was not considered. Even with this much simplified model, excellent agreement between experiment and simulation is observed. The saturation coverage of ~0.9 monolayer, is slightly higher than the experimentally determined saturation coverage of ~0.83 monolayer.

There are no theoretical calculations estimating the CO−CO interaction potential as a function of separation for CO adsorption on Rh{100}. However, information is available for the

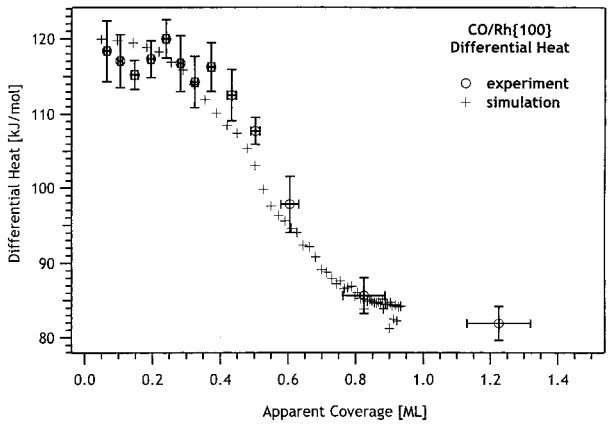

Figure 4. Coverage-dependent differential heats of adsorption determined by the Monte Carlo simulation of CO adsorption on Rh{100} at 300 K.

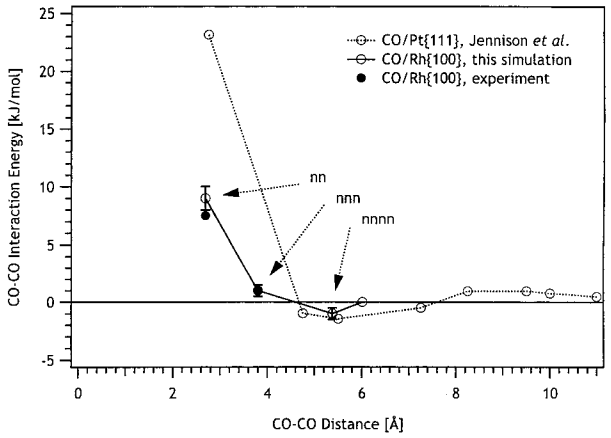

Figure 5. CO−CO interaction potentials for CO/Pt{111}, as determined via DFT calculations by Jennison et al. (dotted curve),[20] and the optimum CO−CO interaction energies from the Monte Carlo simulation (best fit to the experimental data) for the adsorption of CO on Rh{100} (plain line). The error bars indicate the margins within which the simulation produced satisfactory results compared to the experimental data. The filled circles represent the *nn* and *nnn* interaction energies as extracted from the experiment (see text).

CO−CO interaction potential on Pt{111}, determined empirically[19] and theoretically.[20] By means of DFT calculations, Jennison et al. found that the CO−CO interaction potential is oscillatory in nature, with a repulsive energy of 23 kJ mol^{-1} at a separation of 3 Å, rapidly dropping with increasing distance to an attractive interaction energy of −1.45 kJ mol^{-1} at a separation of 5.5 Å. For greater separation, the interaction potential increases again, becoming repulsive, reaches a maximum at ~9 Å, and finally falls to zero for distances above 11 Å. Figure 5 compares this potential with the discrete potential that resulted in the best fit for the Monte Carlo simulation of CO adsorption on Rh{100} and the *nn* and *nnn* interaction energies extracted from the experiment. For this, it was assumed that at a critical coverage between 0.4 and 0.5 monolayer an ordered c(2×2) structure is formed, from which then the *nnn* interaction energies can be estimated. The *nn* interaction energy was determined by taking the difference between the heat of adsorption at ~0.5 monolayer and saturation.

Excellent agreement is achieved when comparing with the experimental data, although gross simplifications are made in the simulation. Comparison with the theoretical data is generally good, with the overall appearance of the potential curve and the reproduction of the oscillatory nature being the most pleasing. One reason for discrepancies will certainly be the

nature of the different metals themselves, but crystal orientation and lattice parameters will also naturally result in a distortion and shift of the potential curve.

4.3. Adsorption Heats. The initial heat of adsorption determined in this experiment (118 ± 4 kJ mol^{-1}) generally is somewhat lower than that from previous TPD studies in which the activation energy of desorption was extracted by various methods. De Jong and Niemantsverdriet determined a zero coverage value of 131 ± 4 kJ mol^{-1} (TPD).[6] Via the study of isothermal desorption of CO with time-resolved electron energy loss spectroscopy (EELS), Wei et al. gain a value of ~135 kJ mol^{-1}.[21] By means of theoretical investigations (density functional theory (DFT)), Hammer et al. calculate a CO−Rh{100} binding energy in the order of 195 kJ mol^{-1} for the bridge-bonded species at 0.25 monolayer in a p(2×2) structure,[22] which is considerably higher than all three experimental measurements. This is the only real discrepancy to date between DFT calculations and calorimetric heats, and usually good agreement between the two is established for a number of adsorbate systems.[22] There is common agreement in the literature that CO binds on-top at low coverages on Rh{100}.[6,8] However, the theoretical calculations demonstrate the high adsorption energy for the bridge site. It is therefore possible that in the experiment the *less stable* on-top site is occupied, with a large activation barrier preventing the occupation of the more stable bridge site. In support of this idea, in recent work, Ge and King[23] have shown, using DFT slab calculations, that there is a significant diffusional barrier between atop and bridge sites on Pt{110}.

5. Summary and Conclusions

The initial heat of adsorption for CO on Rh{100} was measured to be 118 ± 4 kJ mol^{-1}, with an initial sticking probability of ~0.87. Saturation of the surface is achieved at a coverage of ~0.8 monolayer. Upon adsorption, two main adsorbate structures are formed: a c(2×2) structure at 0.5 monolayer and a p($4\sqrt{2}\times\sqrt{2}$)*R*45° structure at 0.75 monolayer. Application of Kisliuk fits gives a Kisliuk parameter of $K = 0.3$ for the first adsorption regime (up to ~0.4 monolayer), whereas adsorption at higher coverages does not seem to be mediated by a precursor state.

Monte Carlo simulations successfully reproduced the differential heat data, giving discrete CO−CO interaction energies of $E_{nn} = 9 \pm 1$ kJ mol^{-1}; $E_{nnn} = 1 \pm 0.5$ kJ mol^{-1}; and $E_{nnnn} = -1 \pm 0.5$ kJ mol^{-1}. Comparison with *nn* and *nnn* interaction energies extracted from the experimental data and with a calculated CO−CO interaction potential for CO on Pt{111}[20] yields excellent overall agreement.

Acknowledgment. Dr. Qingfeng Ge is acknowledged for stimulating discussions. Jacques Chevallier is acknowledged for supplying and mounting the Pt crystals. The Oppenheimer Trust is acknowledged for a studentship (R.K.). Peterhouse, Cambridge, is acknowledged for a Research Fellowship (W.A.B). The EPSRC is acknowledged for an equipment grant.

References and Notes

(1) Brown, W. A.; Kose, R.; King, D. A. *Chem. Rev.* **1998**, *98*, 797−832.
(2) Gurney, B. A.; Lee, J.; Villarubia, J. S.; Ho, W. *J. Chem. Phys.* **1987**, *87*, 6710−6721.
(3) Castner, D. G.; Sexton, B. A.; Somorjai, G. A. *Surf. Sci.* **1978**, *71*, 519−540.
(4) Tucker, C. W., Jr. *J. Appl. Phys.* **1966**, *37*, 3013−3019.
(5) Baraldi, A.; Gregoratti, L.; Comelli, G.; Dhanak, V. R.; Kiskinova, M.; Rosei, R. *Appl. Surf. Sci.* **1996**, *99*, 1−8.
(6) de Jong, A. M.; Niemantsverdriet, J. W. *J. Chem. Phys.* **1994**, *101*, 10126−10133.
(7) Leung, L.-W. H.; He, J.-W.; Goodman, D. W. *J. Chem. Phys.* **1990**, *93*, 8328−8336.
(8) Gurney, B. A.; Richter, L. J.; Villarubia, J. S.; Ho, W. *J. Chem. Phys.* **1987**, *87*, 6710−6721.
(9) Kim, Y.; Peebles, H. C.; White, J. M. *Surf. Sci.* **1982**, *114*, 363−380.
(10) Chan, C.-M.; Aris, R.; Weinberg, W. H. *Appl. Surf. Sci.* **1978**, *1*, 360−376.
(11) de Jong, A. M.; Niemantsverdriet, J. W. *Surf. Sci.* **1990**, *223*, 355−365.
(12) Kisliuk, P. *J. Phys. Chem. Solids* **1957**, *3*, 95−101.
(13) Borroni-Bird, C. E.; King, D. A. *Rev. Sci. Instrum.* **1991**, *62*, 2177−2185.
(14) King, D. A.; Wells, M. G. *Surf. Sci.* **1972**, *29*, 454−482.
(15) Stuck, A.; Wartnaby, C. E.; Yeo, Y. Y.; Stuckless, J. T.; Al-Sarraf, N.; King, D. A. *Surf. Sci.* **1996**, *349*, 229−240.
(16) Metropolis, N.; Rosenbluth, A. W.; Rosenbluth, M. N.; Teller, A. H.; Teller, E. *J. Chem. Phys.* **1953**, *21*, 1087−1092.
(17) Kose, R. New frontiers in single crystal adsortion calorimetry; Thesis, Cambridge University, 1998.
(18) Lide, D. R., Ed. *CRC Handbook of Chemistry and Physics*, 75th ed.; CRC Press: Boca Raton, FL, 1997.
(19) Persson, B. N. J.; Tüshaus, M.; Bradshaw, A. M. *J. Chem. Phys.* **1990**, *92*, 5034−5046.
(20) Jennison, D. R.; Schultz, P. A.; Sears, M. P. *Phys. Rev. Lett.* **1996**, *77*, 4828−4831.
(21) Wei, D. H.; Skelton, D. C.; Kevan, S. D. *Surf. Sci.* **1997**, *381*, 49−64.
(22) Hammer, B.; Hansen, L. B.; Nørskov, J. K. *Phys. Rev. B* **1999**, *59*, 7413.
(23) Ge, Q.; King, D. A. *J. Chem. Phys.* 1999, in press.